A conserved membrane-binding domain targets proteins to organelle contact sites

Alexandre Toulmay and William A. Prinz*

Laboratory of Cell and Molecular Biology, National Institute of Diabetes and Digestive and Kidney Diseases, National Institutes of Health, Bethesda, MD 20892, USA

*Author for correspondence (wprinz@helix.nih.gov)

Accepted 25 July 2011
Journal of Cell Science 125, 49–58

doi: 10.1242/jcs.085118

Summary

Membrane contact sites (MCSs), where the membranes of two organelles are closely apposed, are regions where small molecules such as lipids or calcium are exchanged between organelles. We have identified a conserved membrane-binding domain found exclusively in proteins at MCSs in *Saccharomyces cerevisiae*. The synaptotagmin-like-mitochondrial-lipid binding protein (SMP) domain is conserved across species. We show that all seven proteins that contain this domain in yeast localize to one of three MCSs. Human proteins with SMP domains also localize to MCSs when expressed in yeast. The SMP domain binds membranes and is necessary for protein targeting to MCSs. Proteins containing this domain could be involved in lipid metabolism. This is the first protein domain found exclusively in proteins at MCSs.

Key words: ERMES, Lipid-binding domain, Membrane contact sites, SMP domain

Introduction

The compartmentalization of eukaryotic cells induces the need for inter-organelle communication. One place where this occurs is at membrane contact sites (MCSs), regions where the membranes of two organelles are closely apposed, typically within ~20 nm (Lebiedzinska et al., 2009; Levine and Loewen, 2006; Toulmay and Prinz, 2011). These junctions are found in all cell types and often occur between the endoplasmic reticulum (ER) and a second organelle. They are thought to be sites where lipids (Voelker, 2009) and other small molecules, such as calcium (Lewis, 2007), are exchanged between organelles. The formation of MCSs and how proteins are trafficked to these regions are not well understood.

In the yeast *Saccharomyces cerevisiae* MCSs have been identified between the ER and plasma membrane (PM), the ER and mitochondria, and the nucleus and vacuole (called the nucleus–vacuole junction; NVJ). Protein complexes needed to maintain two of these MCSs are known. NVJ formation requires the interaction of the ER protein Nvj1p and Vac8p on the vacuole, and the NVJ fails to form in cells missing either of these two proteins (Pan et al., 2000). A complex named the ER–mitochondrion encounter structure (ERMES) facilitates contacts between the ER and mitochondria (Kornmann et al., 2009). This complex consists of four proteins: Mdm10p and Mdm34p in the mitochondrial outer membrane, Mmm1p in the ER and the soluble protein Mdm12p. In strains missing any one of these proteins the ERMES complex does not form and the cells have defects in lipid exchange between ER and mitochondria, indicating that the ERMES complex plays a role in maintaining ER–mitochondria contacts (Kornmann et al., 2009).

Three of the four ERMES proteins contain a domain of unknown function called the synaptotagmin-like-mitochondrial-lipid binding protein (SMP) domain (Lee and Hong, 2006). SMP domains are found in membrane-associated proteins from yeast to humans. SMP domains are ~200 amino acids long and were identified by their predicted secondary structure of an alpha helix, four beta strands and a second alpha helix (Lee and Hong, 2006). Most proteins containing SMP domains also have one or more transmembrane domains (TMDs). SMP-containing proteins have been clustered into four groups: C2-containing syntaptotagmin-like proteins, mitochondrial proteins, pleckstrin homology (PH) domain-containing proteins and proteins with C1 domains and PDZ domains. Many PH, C1 and C2 domains bind lipids. Recently, SMP domains were predicted to belong to a superfamily of lipid-binding proteins and form a tube-like structure (Kopec et al., 2010).

In yeast, seven proteins contain SMP domains: Mmm1p, Mdm12p and Mdm34p in the ERMES complex; Tcb1p, Tcb2p and Tcb3p called tricalbins; and the protein encoded by the uncharacterized gene *YPR091C*, which we here name Nvj2p. We show that all the SMP-containing proteins in yeast localize to MCSs, the SMP domain is required for localization, and that SMP domains bind membranes. We also present evidence that all SMP-containing proteins play roles in lipid metabolism.

Results

Nvj2p localizes to the NVJ

Because SMP-containing proteins in the ERMES complex localize to ER–mitochondria contact sites (Kornmann et al., 2009), we wondered whether other proteins that have SMP domains also localize to MCSs. We determined the localization of all the proteins in yeast that contain SMP domains (Fig. 1). One is Nvj2p (encoded by *YPR091C*), a non-essential protein of unknown function. In addition to a SMP domain, Nvj2p contains one putative TMD and a PH domain (Fig. 1). Nvj2p with GFP at its C-terminus has been previously shown to localize to the ER (Huh et al., 2003), a finding we confirmed (Fig. 2A). However, we found that Nvj2–GFP was also enriched on the nuclear membrane

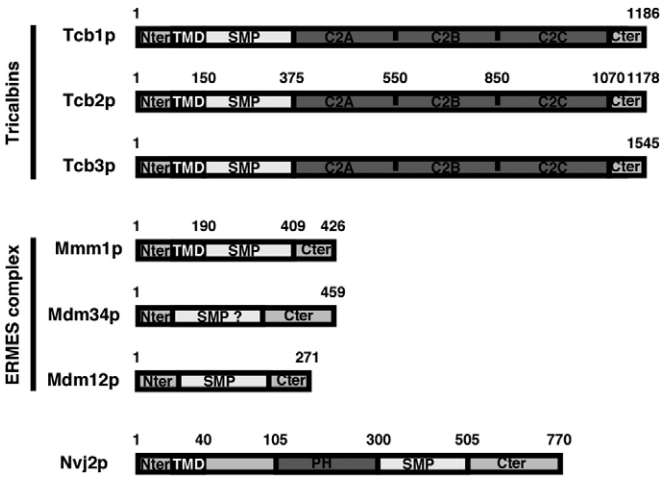

Fig. 1. Diagrams of yeast proteins containing SMP domains. Nterm, N-terminus; Cterm, C-terminus; other abbreviations are as given in the text.

that is apposed to the vacuole, which suggests that it localizes to the NVJ. We confirmed that Nvj2–GFP is at the NVJ by its colocalization with the NVJ marker Nvj1p fused to mCherry (Fig. 2B). In addition, we found that Nvj2–GFP localization to the nuclear membrane that is apposed to the vacuole was abolished in cells missing proteins required for NVJ formation, namely Nvj1p or Vac8p (Fig. 2C) (Pan et al., 2000). Together, these findings show that Nvj2p is enriched at the NVJ.

We found that the extent of enrichment of Nvj2–GFP at the NVJ varied with the growth phase of the cells. In early to mid-logarithmic cultures ~30% of the cells showed weak enrichment of the fusion protein at the NVJ, with a substantial fraction of the fusion protein in other regions of the ER (Fig. 2D, left panels), or strong enrichment of the protein at the NVJ with little in other regions of the ER (Fig. 2D, middle panels). In other cells the fusion protein was uniformly distributed in the ER or in cytoplasmic vesicles. When cells entered late-logarithmic growth phase the percentage of cells with strong enrichment of Nvj2–GFP at the NVJ increases dramatically (Fig. 2E,F). We found that the degree of enrichment of Nvj1–GFP at the NVJ similarly varied with growth phase of cells expressing the fusion protein (supplementary material Fig. S1A–C) and (Pan et al., 2000; Roberts et al., 2003). Thus both Nvj1p and Nvj2p become increasingly enriched at the NVJ as cells enter into late-logarithmic growth phase.

Nvj2p is not required for NVJ formation or piecemeal microautophagy of the nucleus

We investigated whether Nvj2p is required for NVJ formation or localization of other proteins to this domain. Osh1p is a lipid-binding protein that is highly enriched at the NVJ but is not required for NVJ formation (Kvam and Goldfarb, 2004; Levine and Munro, 2001). Targeting of GFP–Osh1p to the NVJ was not altered in cells missing Nvj2p (Fig. 2G). Therefore Nvj2p is not needed for NVJ formation or the localization of another protein to this junction.

In a small fraction of cells expressing Nvj2–GFP the protein was found on vesicles inside of the vacuole (Fig. 2D, right panels). These vesicles probably arise from piecemeal microautophagy of the nucleus (PMN). We cannot exclude that these vesicles also arise from macroautophagy of the ER. Formation of vesicles in the vacuole by PMN occurs at the NVJ and proteins at the NVJ are found on vesicles produced by PMN (Roberts et al., 2003). Cells lacking proteins required for NVJ formation, Nvj1p and Vac8p, or proteins that localize to the NVJ, Osh1p and Tsc13p, have defects in PMN formation (Dawaliby and Mayer, 2010; Kvam et al., 2005; Kvam and Goldfarb, 2004). Therefore we tested weather Nvj2p was also required for PMN. Previous studies have shown that rapamycin induces PMN (Dawaliby and Mayer, 2010; Millen et al., 2009). To assess PMN induction we monitored the internalization of the nucleoplasm protein Pus1–GFP in the vacuole after rapamycin addition. In cells lacking Osh1p or Erg5p PMN induction was substantially reduced compared with that of wild-type cells (supplementary material Fig. S1D,E) (Dawaliby and Mayer, 2010). However, PMN induction was not reduced in cells lacking Nvj2p (supplementary material Fig. S1D,E), suggesting that Nvj2p does not play a significant role in this process. Consistent with this conclusion, we found that Nvj2–GFP localization to the NVJ is not altered in cells lacking Osh1p or lipid-biosynthesis proteins known to reduce PMN, including Elo3p and Erg5p (Dawaliby and Mayer, 2010) (and data not shown). Together these findings suggest that Nvj2p is not required for PMN and that Nvj2p has a function at the NVJ that is not necessary for PMN.

Tricalbins localize to ER–PM contact sites

The tricalbin family of proteins contains an N-terminal TMD and a large C-terminal domain that contains an SMP domain and at least three to six C2 domains (Fig. 1) (Creutz et al., 2004; Jimenez and Davletov, 2007). The C2 domains in tricalbins bind membranes in a calcium-dependent manner (Schulz and Creutz, 2004). The three tricalbins in *S. cerevisiae*, Tcb1p, Tcb2p and Tcb3p, have unknown functions but a mammalian homologue has been implicated in endocytosis (Jean et al., 2010).

Because the tricalbins contain SMP domains we wanted to determine whether they localize to MCSs. The tricalbins have been previously found at the cell periphery (Creutz et al., 2004; Huh et al., 2003). We examined each of the three tricalbins, fused to GFP at their C-termini, in cells that also expressed the ER marker RFP–HDEL. Remarkably, the tricalbins are more enriched in the cortical ER that is closely apposed to the PM than in the perinuclear ER or internal ER tubules that connect the nucleus to the cortical ER (Fig. 3A). This localization is similar to that of the reticulons, which are largely excluded from the perinuclear ER (Voeltz et al., 2006). However, the reticulons are enriched in both the cortical ER and internal ER tubules, whereas the tricalbins are enriched primarily in the cortical ER (supplementary material Fig. S2A). The enrichment of tricalbins in the ER that is closely apposed to the PM is similar to the localization of the oxysterol-binding protein homologues Osh2p, Osh3p, Osh6p and Osh7. It has been suggested that these proteins are enriched at ER–PM contact sites (Loewen et al., 2003; Schulz et al., 2009; Stefan et al., 2011).

The structure of the tricalbins suggests how they might be targeted to regions of the ER closely apposed to the PM; the TMD resides in the ER, and the large soluble domains are cytosolic and can bind the PM. To test this we determined the localization of various portions of Tcb2p fused to GFP (Fig. 3B; supplementary material Fig. S3). We found that a fusion protein containing only the TMD localized to the ER, suggesting that the TMD of Tcb2p resides in this compartment. When the cytosolic portion of Tcb2p was fused to GFP, the resulting fusion protein was targeted to the PM (Fig. 3; supplementary material Fig. S3).

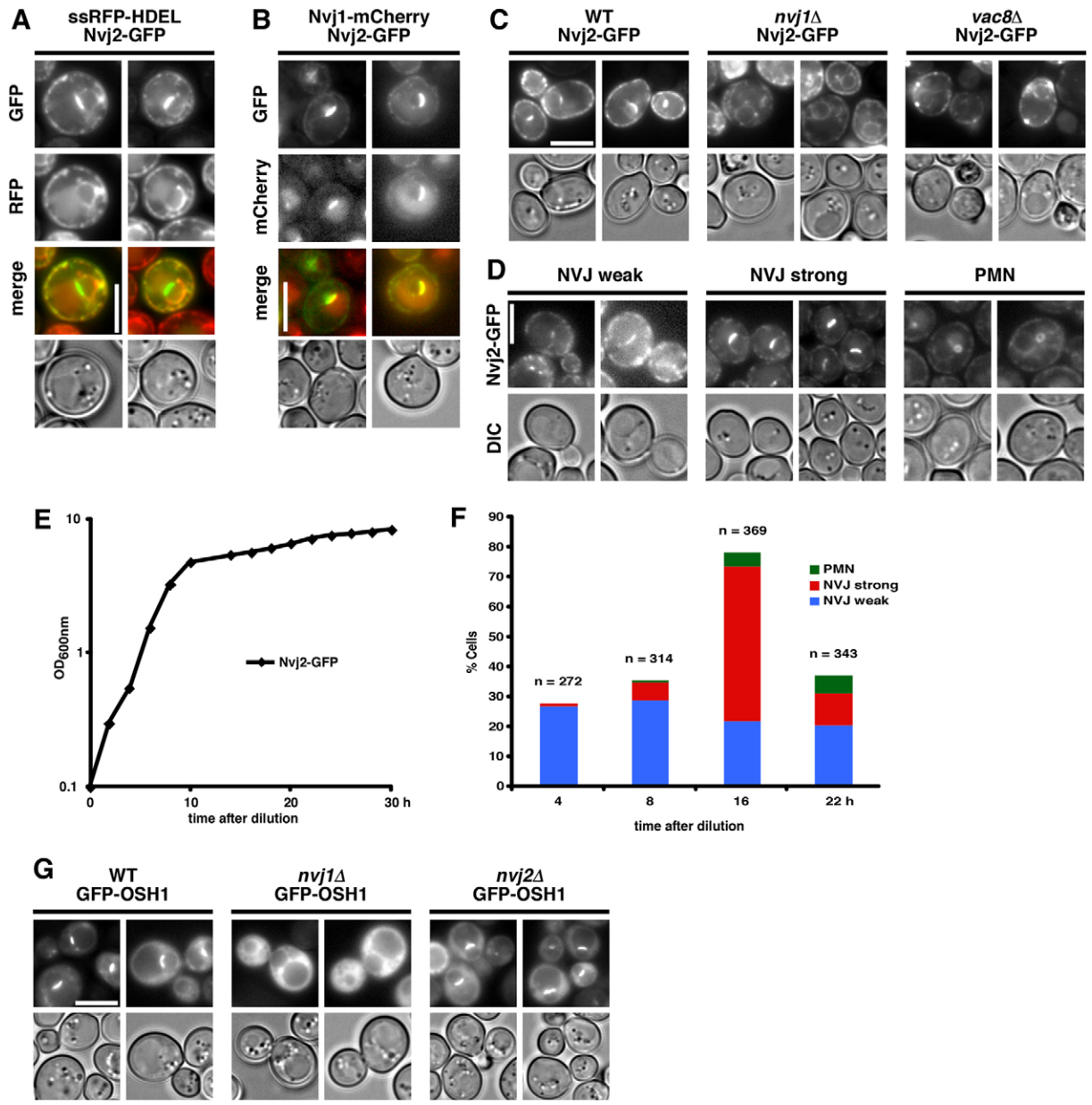

Fig. 2. Nvj2p is localized to NVJ and is not required for NVJ formation. (**A**) Localization of Nvj2–GFP under the *GALl1* promoter expressed for 2 hours in a strain (ATY182) with RFP–HDEL as a marker of the ER. (**B**) Cell expressing Nvj2–GFP and the NVJ marker Nvj1–mCherry (strain ATY192). Nvj2–GFP expression was induced 2 hours before examination. (**C**) Nvj2–GFP under the *GALl1* promoter was expressed for 2 hours in wild-type, *nvj1*Δ and *vac8*Δ yeast strains (ATY192, ATY180 and ATY181, respectively). (**D**) Examples of cells with weak and strong localization of Nvj2–GFP at the NVJ. Cells with Nvj2–GFP localized to PMN blebs and vesicles are also shown. (**E**) Growth curve (measured as the OD at 600 nm) of cells (strain ATY104) expressing Nvj2–GFP and cultured in YPD medium. (**F**) Percentage of cells showing fluorescence at the NVJ and in PMN structures at different time points of the growth curve in E. (**G**) GFP–OSH1, which localizes to the NVJ, expressed in wild-type, *nvj1*Δ and *nvj2*Δ strains (ATY214, ATY183 and ATY187, respectively). Scale bars: 5 µm.

These findings suggest that, similar to Stim1, Stim2, junctionphilins and Ist2p (Deng et al., 2009; Ercan et al., 2009; Fischer et al., 2009; Garbino et al., 2009; Lewis, 2007; Wu et al., 2006), the TMD of Tcb2p is in the ER and its cytosolic domains binds the PM, causing it to be enriched at ER–PM contact sites.

Cortical ER is closely apposed to the PM

The localization of the tricalbins on the ER suggests that they are at ER–PM contact sites. However, these sites are not well defined in yeast and we wanted to estimate how much of the cortical ER is close enough to the PM to allow a protein in the ER to bind a protein in the PM. For these studies we made use of the fact that the Venus fluorescent protein can be made in two parts, called F1 and F2, which can form a functional protein when they interact with each other (MacDonald et al., 2006). To estimate how close the ER and PM come to one another we fused F1 to the C-terminus of the ER membrane protein Sec63p and F2 to the C-terminus of the PM protein Pma1p (Fig. 4A). The C-termini of both proteins are in the cytosol (Ambesi et al., 2000; Feldheim et al., 1992). On the basis of the known structures of Venus and

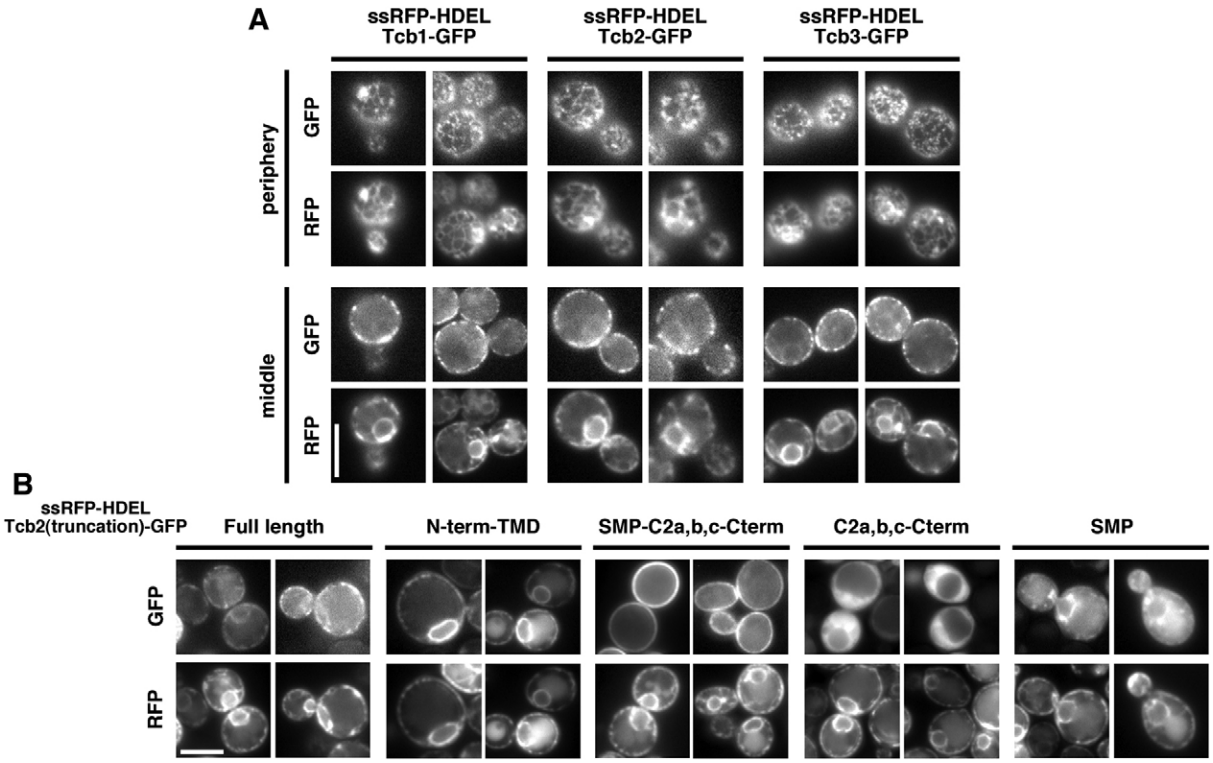

Fig. 3. The tricalbins localize to ER–PM contacts. (**A**) Cells expressing Tcb1–GFP, Tcb2–GFP or Tcb3–GFP and the ER marker RFP–HDEL (strains WPY971, WPY973 and WPY975, respectively). Images were taken focusing on the middle and periphery of the cells. (**B**) Localization of GFP fused to the indicated portions of Tcb2p. The fusion proteins, under the *GALl1* promoter, were expressed for 2 hours in strains containing the ER marker RFP–HDEL (strains ATY33, ATY34, ATY36, ATY37, ATY38). Scale bars: 5 μm.

of the cytosolic tails of homologues of Pma1p and Sec63p (Kuhlbrandt et al., 2002; Rekas et al., 2002; Zhang et al., 2009), we estimated that the ER and PM must come within ~30 nm of one another for Sec63–F2 and Pma1–F1 to form a functional Venus protein. We compared the Venus signal in cells expressing both these fusion proteins with the ER marker RFP–HDEL; Venus colocalized with almost all of the ER that was close to the PM (Fig. 4B, left panels). Thus most of the peripheral ER can come within ~30 nm of the PM. It is possible that the interaction of the ER and PM is driven, in part, by the binding of the two halves of the Venus protein. To see whether the ER and PM could come even closer, we fused F1 to Sec63(1–250), which lacks almost all of the C-terminal cytosolic domain of full-length Sec63p (Fig. 4A). We estimated that for Sec63(1–250)–F1 and Pma1–F2 to form a functional Venus protein the ER and PM must come within ~20 nm of one another. We found that the Venus signal obtained with these proteins colocalized with almost all of the ER marker RFP–HDEL at the cell periphery (Fig. 4B, right panels). Comparable results were also obtained when F2 fused to the PM protein Hxt3p was used in place of Pma1–F2 (not shown). Collectively, these findings suggest that virtually all of the cortical ER can come within ~20 nm of the PM. This is probably a small enough distance that proteins in the ER with large cytosolic domains, such as the tricalbins, could bind the PM.

To confirm that one of the tricalbins can interact with a PM protein we fused F1 to the C-terminus of Tcb2p and expressed this fusion protein with Pma1–F2 (Fig. 4C, left panels). The pattern of Venus fluorescence is similar to that seen with Sec63–F1 and very different from that seen when F1 and F2 are fused to two PM proteins such as Pma1p (Fig. 4C, right panels) or Hxt3p and Pma1p (not shown). Therefore Tcb2p is an ER membrane protein and its C-terminal domain is cytosolic and can interact with the PM.

The enrichment of the tricalbins to ER–PM MCSs suggests that they could maintain the close apposition of the PM and ER. To determine if ER–PM contacts were reduced in cell lacking the tricalbins we determined the percentage of the PM that had ER closely apposed to it. The ER marker Sec63–GFP was expressed in wild-type cells and a strain lacking all three tricalbins. We found that in both strains ~70% of the PM had ER closely apposed with it (supplementary material Fig. S2B), suggesting that the tricalbins are not required to maintain ER–PM contacts. As a second means of determining whether ER–PM contacts are reduced in cells missing the tricalbins, we expressed Sec63–F1 and Pma1–F2 in these cells. We reasoned that if contacts were reduced the F1 and F2 portions of these fusion proteins would not be able to interact and less Venus signal would be observed. However, we found no difference in the intensity of the signal in cells lacking the tricalbins and wild-type cells (supplementary material Fig. S2C). Together, these findings suggest that the tricalbins are not required to maintain PM–ER contact sites.

Human proteins with SMP domains localize to MCSs in yeast

SMP domains are conserved from yeast to humans (Lee and Hong, 2006). We wondered whether human proteins containing SMP domains are enriched at MCSs. Therefore, we investigated

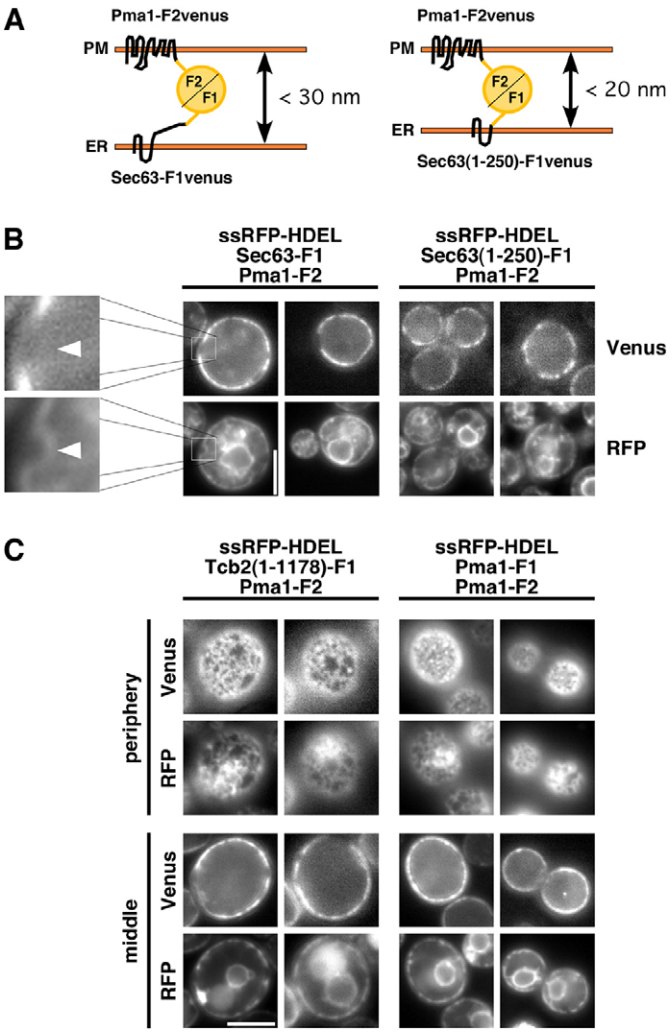

Fig. 4. The cortical ER is closely apposed to the plasma membrane. (**A**) Diagram of the interaction between Sec63-F1 in the ER and Pma1-F2 in the PM. Sec63(1–250)-F1 contains the first 250 amino acids of Sec63p and lacks the C-terminal cytosolic domain of Sec63p. (**B**,**C**) Cells expressing the indicated fusion proteins and the ER marker RFP–HDEL (strains ATY57, ATY98, ATY97, ATY54). Arrowheads indicate peripheral ER that is not close to the PM and lacks Venus signal. The images in C were taken focusing on the middle and periphery of the cells. Scale bars: 5 µm.

whether two of these proteins localize to MCSs when they are expressed in yeast. GFP was fused to the C-terminus of E-Syt1, a tricalbin homologue, which localizes to endomembranes in mammalian cells (Min et al., 2007), and HT008, a homologue of Nvj2p. Both fusion proteins were enriched at MCSs; E-Syt1–GFP localized to ER–PM contacts (Fig. 5A) and HT008–GFP was enriched at the NVJ (Fig. 5B). Therefore, the targeting of SMP-domain-containing proteins to MCSs is conserved and it is possible that all SMP-containing proteins localize to MCSs.

SMP domains target proteins to MCSs

Because SMP-containing proteins localize to MCSs, we determined whether SMP domains are required to target proteins containing them to contact sites. To find which regions of SMP-containing proteins target these proteins to MCS, we fused GFP to portions of Tcb2p, Nvj2p and Mmm1p (Fig. 1).

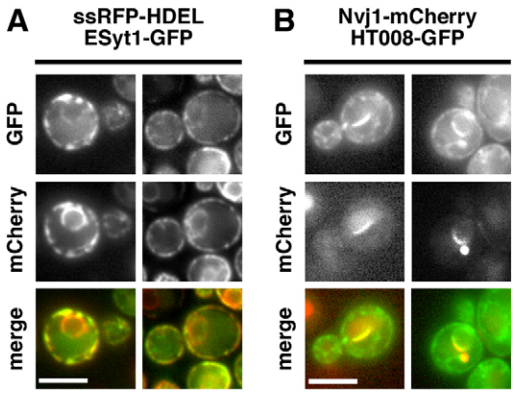

Fig. 5. Human orthologues of the tricalbins and Nvj2p localize to MCSs in yeast. (**A**) The human tricalbin homologue E-Syt1 was fused to GFP and expressed together with the ER marker RFP–HDEL (strain ATY196). (**B**) The human Nvj2p homologue HT008 was fused to GFP and expressed with the NVJ marker Nvj1–mCherry (strain ATY195). Scale bars: 5 µm.

Deletion of the SMP domain from these proteins ablated their MCS localization; instead they were found in all regions of the ER (Fig. 6A–C). Thus the SMP domains of Tcb2p, Nvj2p and Mmm1p are required to target these proteins to MCSs. Other domains are also necessary to target these proteins to MCSs, including their TMDs, at least one C2 domain in Tcb2p and the PH domain in Nvj2p (supplementary material Fig. S3). When only the SMP domains of Tcb2p, Nvj2p or Mmm1p are fused to GFP, the resulting proteins are largely cytosolic, with occasional cytosolic punctae and weak ER fluorescence for the Tcb2 truncation. Taken together, these findings indicate that SMP domains are necessary but not sufficient to localize proteins containing them to MCSs.

As a further test of the ability of SMP domains to target proteins to MCS, we determined if the SMP domains of Tcb2p, Nvj2p, and Mmm1p could target another protein to the MCSs. Tcb2p, Nvj2p and Mmm1p have a single TMD and a large C-terminal soluble domain that includes a SMP domain (Fig. 1). Our findings and previous work (Kornmann et al., 2009) suggests that the TMDs of these proteins are in the ER and their C-terminal domains are cytosolic. We determined if the cytosolic domains of Tcb2p, Nvj2p and Mmm1p could target the ER protein Sec63p to MCSs. Sec63p is an integral membrane protein found all over the ER (Fig. 6D and supplementary material Fig. S2). We removed the N-terminus and TMD (ΔNterm/TMD) of Tcb2p, Nvj2p and Mmm1p and replaced them with Sec63p. All of the resulting fusion proteins were targeted to MCSs: Sec63-Tcb2(ΔNterm/TMD)–GFP to the ER–PM contacts, Sec63-Nvj2(ΔNterm/TMD)–GFP to the NVJ and Sec63-Mmm1(ΔNterm/TMD)–GFP to the ER–mitochondria contacts (Fig. 6D,E). To confirm that Mmm1(ΔNterm/TMD)–GFP is located at ER–mitochondria contacts we determined its colocalization with Mmm1–mCherry (Fig. 6D). Thus, the cytosolic domains of Tcb2p, Nvj2p and Mmm1p, which contain a SMP domain and other domains, can target an integral membrane protein in the ER to MCSs. It is probable that these domains bind the membrane that is apposed to the ER at the MCSs.

SMP domains bind membranes

Because SMP domains are necessary to target proteins to MCSs, we determined whether these domains could bind membranes in

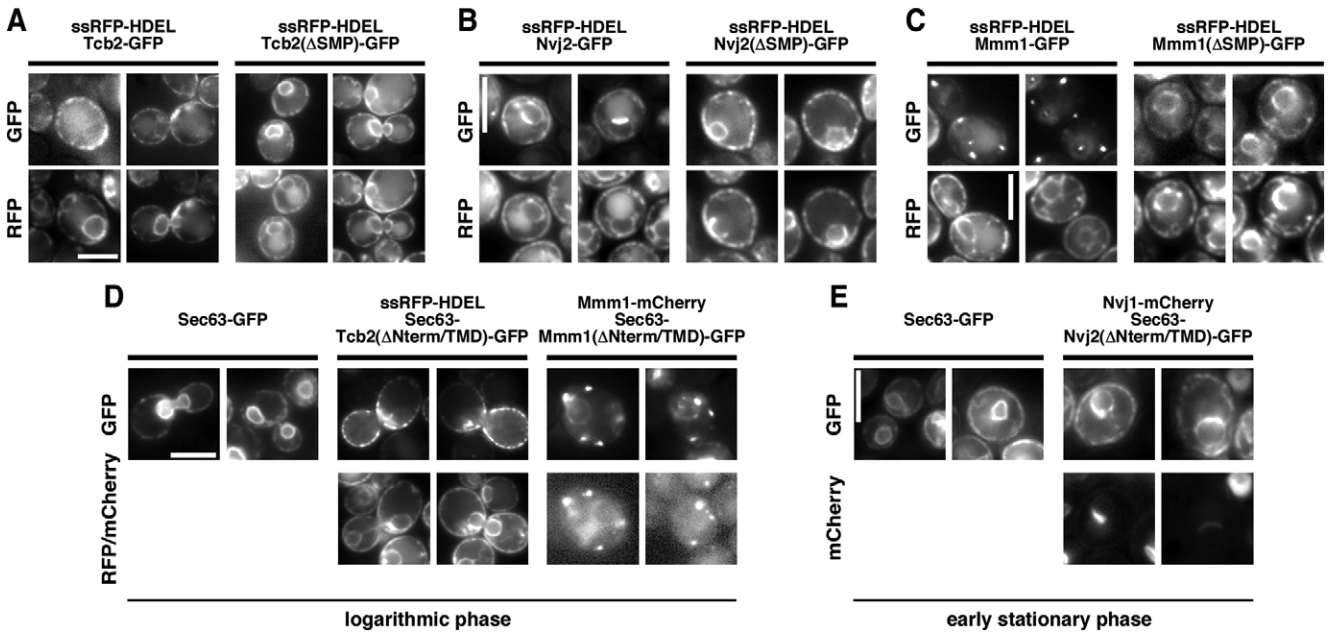

Fig. 6. The SMP domain is necessary for MCS localization. (**A**) Cells expressing either full-length Tcb2–GFP (left panels) or the protein lacking the SMP domain (right panels) and the ER marker RFP–HDEL (strains ATY33 and ATY84, respectively). (**B**) Cells expressing either full-length Nvj2–GFP (left panels) or the protein lacking the SMP domain (right panels) and the ER marker RFP–HDEL (strains ATY182 and ATY250, respectively). (**C**) Cells expressing either full-length Mmm1–GFP (left panels) or the protein lacking the SMP domain (right panels) and the ER marker RFP–HDEL (strains ATY140, ATY142). (**D**,**E**) Images of cells expressing the indicated fusion proteins were coexpressed with the ER marker ssRFP–HDEL, ERMES marker Mmm1–mCherry or the NVJ marker Nvj1–mCherry (strains ATY127, ATY257, ATY218 and ATY217, respectively). Note that the Tcb2p, Mmm1p and Nvj2p portions of the fusions lacked their N-termini and TMDs. Images were taken of cells in mid-logarithmic growth phase (D) or late-logarithmic growth phase (E). In all panels, expression of GFP fusion proteins was induced 2 hours before examination. Scale bars: 5 μm.

vitro. Full-length Mdm12p or the SMP domains of Nvj2p or Tcb2p were fused to maltose-binding protein (MBP), expressed in yeast, and bound to magnetic beads coated with anti-MBP antibody. The beads were then mixed with liposomes with various lipid compositions and trace amounts of [^{3}H]triolein. After washing, the amount of radiolabel bound to the beads was determined. With MBP alone ~3% of the liposomes bound to the beads. The MBP fused to the SMP domains bound two- to five-fold more liposomes (Fig. 7A), indicating that SMP domains bind liposomes. The lipid composition of the liposomes had little effect on the binding ability of MBP–SMP. We also assessed the ability of SMP domains to bind cellular membranes. The SMP domains from Tcb2p, Mmm1p or Nvj2p were fused to GFP and expressed in wild-type cells. Cell lysates were floated in Optiprep gradients. GFP alone was found mostly at the bottom of the gradients, whereas the PM protein Pma1p was in fractions near the top of the gradient (Fig. 7B). The SMP domains fused to GFP were largely in the top fractions of the gradients, indicating that SMP domains bind cellular membranes (Fig. 7B). Interestingly, when cells expressing them were viewed by fluorescence microscopy, these fusion proteins were largely cytosolic (Fig. 3B and supplementary material Fig. S3), suggesting that SMP domains have a low affinity for membranes. Together, these findings indicate that SMP domains can bind membranes, perhaps by interacting directly with lipids.

We wanted to obtain point mutations in a SMP domain that rendered it nonfunctional to determine the role of membrane binding by the SMP domain. We mutagenized conserved residues in the Mdm12p SMP domain but all of the mutations tested retained function (supplementary material Fig. S4).

SMP-domain-containing proteins might modulate lipid metabolism

The functions of SMP-containing proteins are not known. Because cells lacking the ERMES complex (which has three SMP-containing proteins) have defects in lipid exchange between the ER and mitochondria (Kornmann et al., 2009) and the SMP domain has been suggested to bind lipids (Kopec et al., 2010), we wondered if other proteins with SMP domains might also play roles in lipid metabolism. We determined whether cells lacking one or more of the SMP-containing proteins have altered sensitivity to drugs that inhibit lipid biosynthesis. Cells missing one or more of the tricalbins were found to be hypersensitive to myriocin, an inhibitor of serine palmitoyltransferase (the first step in sphingosine biosynthesis; Fig. 8A). Interestingly, a recent systematic screen for protein–lipid interactions found that the tricalbins Tcb2p and Tcb3p bind the sphingolipid precursors phytoceramide and phosphorylated long chain base (Gallego et al., 2010). Thus tricalbins could play roles in sphingolipid metabolism.

We also determined the sensitivity of cells missing one or more of the SMP-containing proteins to fenpropimorph, an inhibitor of ergosterol biosynthesis. Cells missing Nvj2p were found to be more resistant to fenpropimorph than wild-type cells or strains lacking other SMP-containing proteins (Fig. 8B). To determine if the SMP domain in Nvj2p is required for this protein to function we expressed either wild-type Nvj2p or Nvj2p missing the SMP domain in cells lacking endogenous Nvj2p. Cells expressing the wild-type protein were sensitive to fenpropimorph, whereas cells expressing Nvj2p lacking the SMP were not sensitive (supplementary material Fig. S5A),

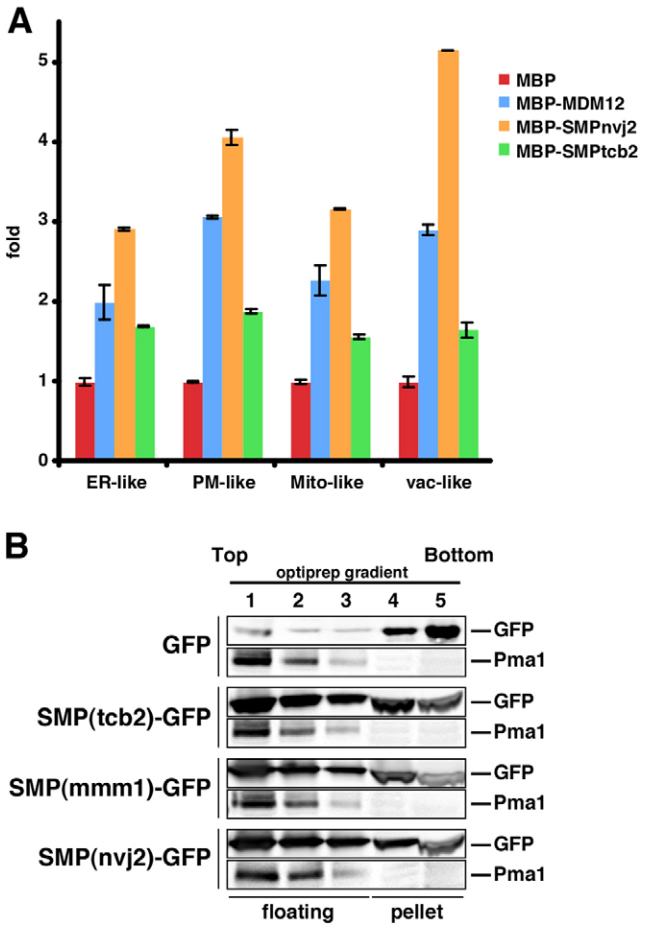

Fig. 7. The SMP domain is a membrane-binding domain. (**A**) MBP fusions to the indicated SMP domains were expressed in yeast and purified on magnetic beads coated with anti-MBP antibody. The amount of protein bound to beads: 10 pmole MBP (in strain ATY287), 4 pmole MBP–Mdm12 (in strain ATY288), 6 pmole MBP–SMP(Nvj2p; in strain ATY290), and 0.2 pmole MBP–SMP(Tcb2p; in strain ATY289). The beads were mixed with liposomes with various lipid compositions and trace [^{3}H]triolein for 30 minutes at 30℃ (mol% of liposomes: ER-like, PC:PS:PE:PI, 50:10:30:10; PM-like, PC:PS:PE:PI:PtdIns(4,5)P_2:cholesterol, 12:28:20:20:1:20; mitochondria-like, PC:CL:PE:PI, 50:10:30:10; vacuole-like, PC:PS:PE:PI:PtdIns(3,5)P_2, 50:5:22.5:22.5:1). The beads were washed twice and counted in a scintillation counter. The counts per minute were normalized to that of the MBP sample. (**B**) Lysates from yeast strains expressing the indicated SMP domains fused to GFP were separated on Optiprep gradients as described in Materials and Methods. Five equal fractions were taken from the top (fraction 1) to the bottom (fraction 5) of the gradient and immunoblotted with antibodies against GFP and the PM proteins Pma1p (strains ATY1, ATY38, ATY153, ATY135). PC, phosphatidylcholine; PE, phosphatidylethanolamine; PI, phosphatidylinositol; PtdIns(3,5)P_2, phosphatidylinositol (3,5)-bisphosphate; PtdIns(4,5)P_2, phosphatidylinositol (4,5)-bisphosphate; PS, phosphatidyl serine.

indicating that the SMP domain in Nvj2p is required for proper function. A role for Nvj2p in ergosterol metabolism is also suggested by the finding that it binds ergosterol in lipid arrays (Gallego et al., 2010). Because cells missing Nvj2p are resistant to fenpropimorph, we tested whether cells missing other NVJ proteins, or those involved in PMN formation, were also resistant. Cells missing Nvj1p were not resistant (supplementary material Fig. S5B). Interestingly, cells missing Osh1p, another

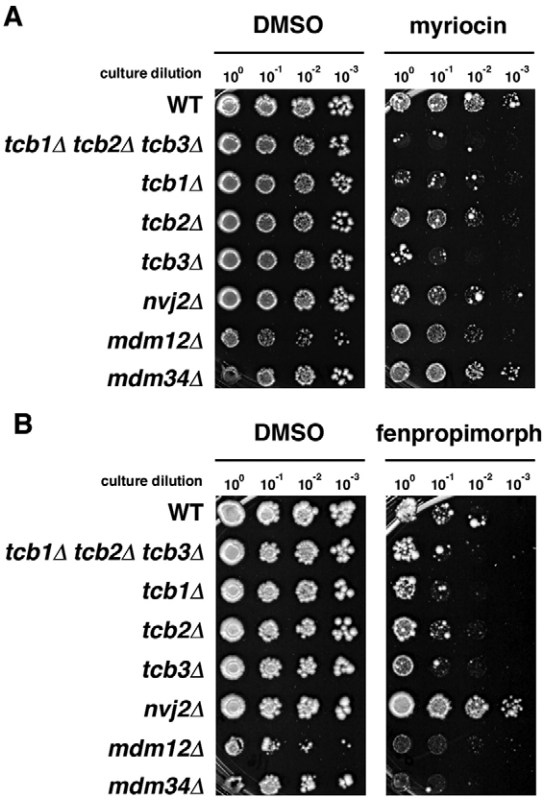

Fig. 8. Sensitivity of cells missing SMP-containing proteins to lipid biosynthesis inhibitors. Cultures of the indicated strains were grown to mid-logarithmic growth phase in YPD and adjusted to OD_{600nm}=1. Serial tenfold dilutions were spotted on (**A**) SC plates containing the indicated concentrations of myriocin and (**B**) YPD plates with the indicated concentrations of fenpropimorph. The plates were incubated for 4 days at 30℃. (Strains BY4741, ATY109, ATY291, ATY292, ATY293, ATY294, WPY267 and CVY551).

ergosterol-binding protein that localizes to the NVJ, were also found to be resistant to fenpropimorph (supplementary material Fig. S5B). Similarly, cells missing Elo3p, another protein involved in PMN formation, are resistant to fenpropimorph as well (supplementary material Fig. S5B). These findings suggest that Nvj2p and Osh1p function in sterol metabolism or signaling at the NVJ.

Discussion

We found that all the seven proteins in yeast that contain a SMP domain are enriched at MCSs. This is the first domain found exclusively in proteins at MCSs in yeast. Two human proteins containing SMP domains, E-Syt1 and HT008, also localized to MCSs when expressed in yeast, suggesting that all proteins containing SMP domains have an affinity for MCSs. Our efforts to identify the location of E-Syt1 and HT008 in mammalian cells using GFP fusions were not successful but the fact that these proteins localize to MCSs in yeast suggests that they are enriched at these sites in mammalian cells as well. However, it should be noted that although we found E-Syt1 at ER–PM contacts in yeast, a previous study found that this protein localized to endomembranes in HEK293 cells and the E-Syt1 homologues E-Syt2 and E-Syt3 were found on the PM (Min et al., 2007). It might be that E-Syt proteins and some other mammalian proteins

with SMP domains are recruited to MCSs only in some circumstances or that not all mammalian proteins with SMP domains are enriched at MCSs.

Many of the SMP-containing proteins in yeast have a single TMD that is probably in the ER. It seems likely that the cytosolic portions of these proteins, which include the SMP domain, interact with the membrane that is apposed to the ER at MCSs and this interaction is required to enrich these proteins at MCSs. We found that SMP domains bind membranes and are required to target proteins containing these domains to MCSs. SMP domains were found to have little specificity for particular lipids because they bound about as well to liposomes with different lipid compositions. SMP domains also seem to have a low affinity for membranes. When SMP domains were fused to GFP they were largely cytosolic but floated with membranes in Optiprep gradients. The ability of SMP domains to bind membranes probably helps target proteins containing these domains to MCSs.

We suspect that SMP domains not only target proteins to MCSs but also have functions that are unique to proteins at MCSs. For example, they might maintain a specific distance between the membranes at MCSs, assist the exchange of small molecules between organelles or participate in signaling reactions that occur at MCSs (supplementary material Fig. S6). Interestingly, it has recently been proposed that SMP forms a conduit that allows lipid exchange between apposed membranes (Kopec et al., 2010). Thus ERMES proteins with SMP domains might facilitate lipid exchange between the ER and mitochondria, and it has been shown that lipid transfer between these organelles slows in mutants missing the ERMES complex (Kornmann et al., 2009). We have found that mutants missing other SMP-containing proteins have altered sensitivities to drugs that inhibit lipid biosynthesis. Therefore, in yeast all proteins with SMP domains might play roles in lipid metabolism, trafficking or signaling. Solving the structure of a SMP domain could yield important clues about how these domains function.

Our work has revealed that a substantial portion of the peripheral ER can come close enough to the PM that proteins in the two membranes can interact. This finding is consistent with a study of ER structure by electron microscopy using chemically fixed cells that found >1000 ER–PM contact per cell (Pichler et al., 2001). However, a subsequent investigation that used high-pressure fixation found only ten ER–PM contacts per cell (Perktold et al., 2007). A more recent study of yeast ER structure using tomography found the mean distance between the cortical ER and PM to be 33 nm and that there are extensive regions of ER–PM contact; 25–40% of the cytoplasmic face of the PM has closely apposed ER (West et al., 2011). This suggests that a substantial portion of the ER is closely apposed to the PM, consistent with our findings. Interestingly, we found that Sec63(1–250)-F1 and Pma1-F2, which probably require the PM and ER to come within ~20 nm of each other to interact, still bound and formed a functional Venus protein. This suggests that contacts between the ER and PM are dynamic and the distance between these organelles is not constant. How close contacts between the PM and ER are maintained is not well understood. None of the proteins that have so far been located at the ER–PM contacts in yeast, including the tricalbins in this work, is required to maintain contacts. It seems probable that contacts are maintained by many low affinity, dynamic interactions rather than by a single, highly abundant protein complex. This could explain why the ER and PM, despite extensive regions of close contact, are not maintained at a fixed distance.

We have found that the previously uncharacterized gene *YPR091C* encodes a protein that localizes to the NVJ and that we have named Nvj2p. This is the fifth protein found to reside at this MCS. The function of the NVJ is unclear but is known to play a role in PMN formation. Interestingly, Nvj2p is the first protein known to be located at the NVJ that is not needed for PMN induction. Therefore the NVJ probably has a function other than autophagy of the nucleus, which could be exchange of lipids or calcium between the nucleus and vacuole. We found that cells missing Nvj2p are resistant to the ergosterol biosynthesis inhibitor fenpropimorph. Interestingly, we have found that cells missing Osh1p, a sterol-binding protein located at the NVJ, are also resistant to fenpropimorph (supplementary material Fig. S5B). The genes encoding Osh1p and Nvj2p have a co-fitness interaction (Hillenmeyer et al., 2008) and genetically interact with the ergosterol biosynthesis gene *ERG11* (Kohl et al., 2010). Mutations in *ERG11* also cause fenpropimorph resistance (Lorenz and Parks, 1991). Together, these findings suggest that Osh1p and Nvj2p participate in a sterol trafficking or signaling pathway at the NVJ. It is notable that some proteins required for the synthesis of long chain fatty acids, needed for sphingolipid biosynthesis, localize to the NVJ and are needed for PMN formation. Mutations in one of these proteins, FEN1 (also known as ELO2; a fatty acid elongase), cause cells to become fenpropimorph resistant (Ladeveze et al., 1993; Lorenz and Parks, 1991). The Mayer group has found that some fatty acid elongases are involved in PMN formation (Dawaliby and Mayer, 2010; Kvam et al., 2005). We found that cells lacking Elo3p are also resistant to fenpropimorph (supplementary material Fig. S4A). Together, these findings suggest that sterols and sphingolipids play important roles in NVJ function and PMN formation. What role SMP domains play in these processes and in the regulation of lipid metabolism by other SMP-containing proteins remains an important question for the future.

Materials and Methods

Strains and plasmids

The strains and plasmids used are listed in supplementary material Table S1.

Fluorescence microscopy

Unless noted, cells were grown in synthetic complete (SC) medium (0.67% yeast nitrogen base and 2% glucose). Live cells in logarithmic phase were viewed using a BX61 microscope (Olympus) with an UPlan Apo 100×/1.35 NA lens, a camera Retiga EX (QImaging) and IVision software (version 4.0.5; BioVision Technologies). Strains containing plasmids with the *GALl1* promoter were grown in SC medium with 2% raffinose instead of glucose and then shifted to SC with 1% raffinose and 2% galactose 2 hours before examination.

Liposome binding assay

Wild-type yeast cells expressing MBP–SMP fusions were grown to mid-logarithmic phase and lysed by agitation with glass beads in Mini-BeadBeater-8 (Biospec Products). The cell lysates (from four OD_{600nm} units of culture) were mixed with magnetic beads coated with 400 µg anti-MBP antibody (New England Biolabs) for 1 hour on ice and mixed every 15 minutes. The beads were washed twice with antibody buffer (0.1 M sodium phosphate, pH 8), then twice with antibody buffer with 0.1% NP-40, and twice with the liposome buffer (20 mM HEPES pH 7.3, 100 mM NaCl, 1 mM EDTA). Liposomes with various lipid composition and a trace amount of [^{3}H]triolein (American Radiolabled Chemicals) were added to the magnetic beads to a final concentration of 1 mM in a total volume 100 µl and incubated at 30℃ for 30 minutes. The beads were washed twice with liposome buffer at 4℃ and counted in a scintillation counter. A portion of the beads was used to estimate the amount of MBP fusion protein bound to them. The beads were mixed with 2× SDS sample buffer and proteins bound were separated by SDS-PAGE. The amount of MBP fusion protein was determined by

immunoblotting with anti-MBP antibody (New England Biolabs) and comparing the results with those of known amounts of pure MBP.

Membrane flotation in Optiprep gradients

Membranes were floated on Optiprep gradients using a method adapted from Bagnat et al. (Bagnat et al., 2000). Cells expressing GFP fusion proteins under the *GAL1* promoter were induced for 3 hours in medium with galactose and lysed by agitation with glass beads in TNE (30 mM Tris pH 7.5, 150 mM NaCl, 5 mM EDTA) with proteinase inhibitors (Roche). The lysates were spun at 500 ***g*** for 5 minutes at 4℃ to remove unlysed cells and debris. Lysate from ~15 OD_{600nm} units of cells was mixed with Optiprep to yield a final concentration of 40% of Optiprep in a volume of 0.84 ml. The samples were loaded at the bottom a centrifuge tube and overlayed with 1.14 ml of 30% Optiprep in TNE and 0.22 ml of TNE and centrifuged at 100,000 ***g*** for 2.5 hours at 4℃. Five fractions were collected from the top to the bottom of the gradient and trichloroacetic acid was added to 10%. The fractions were separated by SDS-PAGE and immunoblotted with antibodies against GFP (Roche) and yeast Pma1p (kindly provided by Ramón Serrano, Universidad Politecnica de Valencia-CSIC, Valencia, Spain).

Lipid synthesis inhibitor drug assays

Logarithmic yeast cultures were adjusted to $OD_{600nm}=1$ and a series of tenfold dilutions were prepared. The dilutions were spotted on YPD plates containing either DMSO or fenpropimorph (Sigma-Aldrich) at concentration of 1.25 µM or 7.5 µM. The dilutions were also spotted on SC medium plates containing either DMSO or myriocin (Sigma-Aldrich) at a concentration of 0.5 µg/ml.

PMN induction assay

PMN formation was induced using a method adapted from that of Dawaliby and Mayer (Dawaliby and Mayer, 2010). Cultures of cells expressing Pus1–GFP were grown in SC medium to early logarithmic phase, 10 µM FM4-64 was added to the medium, and the cells were grown for 1 hour at 30℃. The cultures were then washed twice with FM4-64-free medium and resuspended in SC medium to an OD_{600nm} of 0.4. After growth for 1 hour at 30℃, 0.2 µM rapamycin (Enzo Life Sciences) or DMSO and 1 mM PMSF were added to the medium, and PMSF was added again to the medium every hour until the cells were harvested. After 4 hours the cells were examined by fluorescence microscopy.

Acknowledgements

We thank T. Levine, O. Cohen-Fix, C. Loewen, J. Nunnari and C. Voss for plasmids and strains and O. Cohen-Fix and A. Slack for critically reading the manuscript.

Funding

This work was supported by the Intramural Research Program of the National Institute of Diabetes and Digestive and Kidney Diseases.

Supplementary material available online at
http://jcs.biologists.org/lookup/suppl/doi:10.1242/jcs.085118/-/DC1

References

Ambesi, A., Miranda, M., Petrov, V. V. and Slayman, C. W. (2000). Biogenesis and function of the yeast plasma-membrane H(+)-ATPase. *J. Exp. Biol.* **203**, 155-160.

Bagnat, M., Keranen, S., Shevchenko, A., Shevchenko, A. and Simons, K. (2000). Lipid rafts function in biosynthetic delivery of proteins to the cell surface in yeast. *Proc. Natl. Acad. Sci. USA* **97**, 3254-3259.

Creutz, C. E., Snyder, S. L. and Schulz, T. A. (2004). Characterization of the yeast tricalbins: membrane-bound multi-C2-domain proteins that form complexes involved in membrane trafficking. *Cell Mol. Life Sci.* **61**, 1208-1220.

Dawaliby, R. and Mayer, A. (2010). Microautophagy of the nucleus coincides with a vacuolar diffusion barrier at nuclear-vacuolar junctions. *Mol. Biol. Cell* **21**, 4173-4183.

Deng, X., Wang, Y., Zhou, Y., Soboloff, J. and Gill, D. L. (2009). STIM and Orai: dynamic intermembrane coupling to control cellular calcium signals. *J. Biol. Chem.* **284**, 22501-22505.

Ercan, E., Momburg, F., Engel, U., Temmerman, K., Nickel, W. and Seedorf, M. (2009). A conserved, lipid-mediated sorting mechanism of yeast Ist2 and mammalian STIM proteins to the peripheral ER. *Traffic* **10**, 1802-1818.

Feldheim, D., Rothblatt, J. and Schekman, R. (1992). Topology and functional domains of Sec63p, an endoplasmic reticulum membrane protein required for secretory protein translocation. *Mol. Cell Biol.* **12**, 3288-3296.

Fischer, M. A., Temmerman, K., Ercan, E., Nickel, W. and Seedorf, M. (2009). Binding of plasma membrane lipids recruits the yeast integral membrane protein Ist2 to the cortical ER. *Traffic* **10**, 1084-1097.

Gallego, O., Betts, M. J., Gvozdenovic-Jeremic, J., Maeda, K., Matetzki, C., Aguilar-Gurrieri, C., Beltran-Alvarez, P., Bonn, S., Fernandez-Tornero, C., Jensen, L. J. et al. (2010). A systematic screen for protein-lipid interactions in Saccharomyces cerevisiae. *Mol. Syst. Biol.* **6**, 430.

Garbino, A., van Oort, R. J., Dixit, S. S., Landstrom, A. P., Ackerman, M. J. and Wehrens, X. H. (2009). Molecular evolution of the junctophilin gene family. *Physiol. Genomics* **37**, 175-186.

Hillenmeyer, M. E., Fung, E., Wildenhain, J., Pierce, S. E., Hoon, S., Lee, W., Proctor, M., St Onge, R. P., Tyers, M., Koller, D. et al. (2008). The chemical genomic portrait of yeast: uncovering a phenotype for all genes. *Science* **320**, 362-365.

Huh, W. K., Falvo, J. V., Gerke, L. C., Carroll, A. S., Howson, R. W., Weissman, J. S. and O'Shea, E. K. (2003). Global analysis of protein localization in budding yeast. *Nature* **425**, 686-691.

Jean, S., Mikryukov, A., Tremblay, M. G., Baril, J., Guillou, F., Bellenfant, S. and Moss, T. (2010). Extended-synaptotagmin-2 mediates FGF receptor endocytosis and ERK activation in vivo. *Dev. Cell* **19**, 426-439.

Jimenez, J. L. and Davletov, B. (2007). Beta-strand recombination in tricalbin evolution and the origin of synaptotagmin-like C2 domains. *Proteins* **68**, 770-778.

Koh, J. L., Ding, H., Costanzo, M., Baryshnikova, A., Toufighi, K., Bader, G. D., Myers, C. L., Andrews, B. J. and Boone, C. (2010). DRYGIN: a database of quantitative genetic interaction networks in yeast. *Nucleic Acids. Res.* **38**, D502-D507.

Kopec, K. O., Alva, V. and Lupas, A. N. (2010). Homology of SMP domains to the TULIP superfamily of lipid-binding proteins provides a structural basis for lipid exchange between ER and mitochondria. *Bioinformatics* **26**, 1927-1931.

Kornmann, B., Currie, E., Collins, S. R., Schuldiner, M., Nunnari, J., Weissman, J. S. and Walter, P. (2009). An ER-mitochondria tethering complex revealed by a synthetic biology screen. *Science* **325**, 477-481.

Kuhlbrandt, W., Zeelen, J. and Dietrich, J. (2002). Structure, mechanism, and regulation of the Neurospora plasma membrane H+-ATPase. *Science* **297**, 1692-1696.

Kvam, E. and Goldfarb, D. S. (2004). Nvj1p is the outer-nuclear-membrane receptor for oxysterol-binding protein homolog Osh1p in *Saccharomyces cerevisiae. J. Cell Sci.* **117**, 4959-4968.

Kvam, E., Gable, K., Dunn, T. M. and Goldfarb, D. S. (2005). Targeting of Tsc13p to nucleus-vacuole junctions: a role for very-long-chain fatty acids in the biogenesis of microautophagic vesicles. *Mol. Biol. Cell* **16**, 3987-3998.

Ladeveze, V., Marcireau, C., Delourme, D. and Karst, F. (1993). General resistance to sterol biosynthesis inhibitors in Saccharomyces cerevisiae. *Lipids* **28**, 907-912.

Lebiedzinska, M., Szabadkai, G., Jones, A. W., Duszynski, J. and Wieckowski, M. R. (2009). Interactions between the endoplasmic reticulum, mitochondria, plasma membrane and other subcellular organelles. *Int. J. Biochem. Cell Biol.* **41**, 1805-1816.

Lee, I. and Hong, W. (2006). Diverse membrane-associated proteins contain a novel SMP domain. *FASEB J.* **20**, 202-206.

Levine, T. and Loewen, C. (2006). Inter-organelle membrane contact sites: through a glass, darkly. *Curr. Opin. Cell Biol.* **18**, 371-378.

Levine, T. P. and Munro, S. (2001). Dual targeting of Osh1p, a yeast homologue of oxysterol-binding protein, to both the Golgi and the nucleus-vacuole junction. *Mol. Biol. Cell* **12**, 1633-1644.

Lewis, R. S. (2007). The molecular choreography of a store-operated calcium channel. *Nature* **446**, 284-287.

Loewen, C. J., Roy, A. and Levine, T. P. (2003). A conserved ER targeting motif in three families of lipid binding proteins and in Opi1p binds VAP. *EMBO J.* **22**, 2025-2035.

Lorenz, R. T. and Parks, L. W. (1991). Physiological effects of fenpropimorph on wild-type Saccharomyces cerevisiae and fenpropimorph-resistant mutants. *Antimicrob. Agents Chemother.* **35**, 1532-1537.

MacDonald, M. L., Lamerdin, J., Owens, S., Keon, B. H., Bilter, G. K., Shang, Z., Huang, Z., Yu, H., Dias, J., Minami, T. et al. (2006). Identifying off-target effects and hidden phenotypes of drugs in human cells. *Nat. Chem. Biol.* **2**, 329-337.

Millen, J. I., Krick, R., Prick, T., Thumm, M. and Goldfarb, D. S. (2009). Measuring piecemeal microautophagy of the nucleus in Saccharomyces cerevisiae. *Autophagy* **5**, 75-81.

Min, S. W., Chang, W. P. and Sudhof, T. C. (2007). E-Syts, a family of membranous Ca2+-sensor proteins with multiple C2 domains. *Proc. Natl. Acad. Sci. USA* **104**, 3823-3828.

Pan, X., Roberts, P., Chen, Y., Kvam, E., Shulga, N., Huang, K., Lemmon, S. and Goldfarb, D. S. (2000). Nucleus-vacuole junctions in Saccharomyces cerevisiae are formed through the direct interaction of Vac8p with Nvj1p. *Mol. Biol. Cell* **11**, 2445-2457.

Perktold, A., Zechmann, B., Daum, G. and Zellnig, G. (2007). Organelle association visualized by three-dimensional ultrastructural imaging of the yeast cell. *FEMS Yeast Res.* **7**, 629-638.

Pichler, H., Gaigg, B., Hrastnik, C., Achleitner, G., Kohlwein, S. D., Zellnig, G., Perktold, A. and Daum, G. (2001). A subfraction of the yeast endoplasmic reticulum associates with the plasma membrane and has a high capacity to synthesize lipids. *Eur. J. Biochem.* **268**, 2351-2361.

Rekas, A., Alattia, J. R., Nagai, T., Miyawaki, A. and Ikura, M. (2002). Crystal structure of venus, a yellow fluorescent protein with improved maturation and reduced environmental sensitivity. *J. Biol. Chem.* **277**, 50573-50578.

Roberts, P., Moshitch-Moshkovitz, S., Kvam, E., O'Toole, E., Winey, M. and Goldfarb, D. S. (2003). Piecemeal microautophagy of nucleus in Saccharomyces cerevisiae. *Mol. Biol. Cell* **14**, 129-141.

Schulz, T. A. and Creutz, C. E. (2004). The tricalbin C2 domains: lipid-binding properties of a novel, synaptotagmin-like yeast protein family. *Biochemistry* **43**, 3987-3995.

Schulz, T. A., Choi, M. G., Raychaudhuri, S., Mears, J. A., Ghirlando, R., Hinshaw, J. E. and Prinz, W. A. (2009). Lipid-regulated sterol transfer between closely apposed membranes by oxysterol-binding protein homologues. *J. Cell Biol.* **187**, 889-903.

Stefan, C. J., Manford, A. G., Baird, D., Yamada-Hanff, J., Mao, Y. and Emr, S. D. (2011). Osh proteins regulate phosphoinositide metabolism at ER-plasma membrane contact sites. *Cell* **144**, 389-401.

Toulmay, A. and Prinz, W. A. (2011). Lipid transfer and signaling at organelle contact sites: the tip of the iceberg. *Curr. Opin. Cell Biol.* **23**, 458-463.

Voelker, D. R. (2009). Genetic and biochemical analysis of non-vesicular lipid traffic. *Annu. Rev. Biochem.* **78**, 827-856.

Voeltz, G. K., Prinz, W. A., Shibata, Y., Rist, J. M. and Rapoport, T. A. (2006). A class of membrane proteins shaping the tubular endoplasmic reticulum. *Cell* **124**, 573-586.

West, M., Zurek, N., Hoenger, A. and Voeltz, G. K. (2011). A 3D analysis of yeast ER structure reveals how ER domains are organized by membrane curvature. *J. Cell Biol.* **193**, 333-346.

Winzeler, E. A., Shoemaker, D. D., Astromoff, A., Liang, H., Anderson, K., Andre, B., Bangham, R., Benito, R., Boeke, J. D., Bussey, H. et al. (1999). Functional characterization of the S. cerevisiae genome by gene deletion and parallel analysis. *Science* **285**, 901-906.

Wu, M. M., Buchanan, J., Luik, R. M. and Lewis, R. S. (2006). Ca2+ store depletion causes STIM1 to accumulate in ER regions closely associated with the plasma membrane. *J. Cell Biol.* **174**, 803-813.

Zhang, L., Xu, T., Maeder, C., Bud, L. O., Shanks, J., Nix, J., Guthrie, C., Pleiss, J. A. and Zhao, R. (2009). Structural evidence for consecutive Hel308-like modules in the spliceosomal ATPase Brr2. *Nat. Struct. Mol. Biol.* **16**, 731-739.